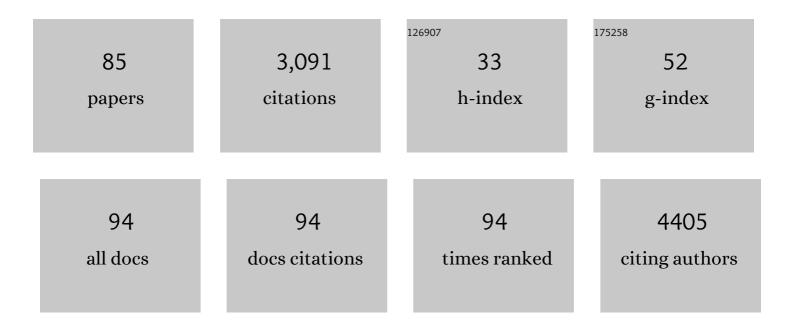
Gisela E Hagberg

List of Publications by Year in descending order

Source: https://exaly.com/author-pdf/8223152/publications.pdf Version: 2024-02-01



CISELA E HACREDO

#	Article	IF	CITATIONS
1	Perception is associated with the brainâ \in Ms metabolic response to sensory stimulation. ELife, 2022, 11, .	6.0	11
2	Developing formalinâ€based fixative agents for post mortem brain MRI at 9.4ÂT. Magnetic Resonance in Medicine, 2022, 87, 2481-2494.	3.0	5
3	Microvascular imaging of the unstained human superior colliculus using synchrotron-radiation phase-contrast microtomography. Scientific Reports, 2022, 12, .	3.3	4
4	Phaseâ€based masking for quantitative susceptibility mapping of the human brain at 9. <scp>4T</scp> . Magnetic Resonance in Medicine, 2022, 88, 2267-2276.	3.0	7
5	T2-Pseudonormalization and Microstructural Characterization in Advanced Stages of Late-infantile Metachromatic Leukodystrophy. Clinical Neuroradiology, 2021, 31, 969-980.	1.9	10
6	Multiâ€echo gradientâ€recalledâ€echo phase unwrapping using a Nyquist sampled virtual echo train in the presence of highâ€field gradients. Magnetic Resonance in Medicine, 2021, 86, 2220-2233.	3.0	1
7	Quantitative Susceptibility Mapping of the Basal Ganglia and Thalamus at 9.4 Tesla. Frontiers in Neuroanatomy, 2021, 15, 725731.	1.7	2
8	Disturbed Balance of Inhibitory Signaling Links Hearing Loss and Cognition. Frontiers in Neural Circuits, 2021, 15, 785603.	2.8	11
9	Depth relationships and measures of tissue thickness in dorsal midbrain. Human Brain Mapping, 2020, 41, 5083-5096.	3.6	4
10	Ultra-High Field MRI in Alzheimer's Disease: Effective Transverse Relaxation Rate and Quantitative Susceptibility Mapping of Human Brain In Vivo and Ex Vivo compared to Histology. Journal of Alzheimer's Disease, 2020, 73, 1481-1499.	2.6	24
11	In-vivo quantitative structural imaging of the human midbrain and the superior colliculus at 9.4T. NeuroImage, 2018, 177, 117-128.	4.2	11
12	[I004] Diffusion-weighted MRI: Techniques, applications and challenges in oncology. Physica Medica, 2018, 52, 2.	0.7	0
13	Depthâ€dependence of visual signals in the human superior colliculus at 9.4 T. Human Brain Mapping, 2017, 38, 574-587.	3.6	11
14	"Wrong Way Up― Temporal and Spatial Dynamics of the Networks for Body Motion Processing at 9.4 T. Cerebral Cortex, 2017, 27, 5318-5330.	2.9	21
15	Whole brain MP2RAGE-based mapping of the longitudinal relaxation time at 9.4T. NeuroImage, 2017, 144, 203-216.	4.2	40
16	Assessing White Matter Microstructure in Brain Regions with Different Myelin Architecture Using MRI. PLoS ONE, 2016, 11, e0167274.	2.5	37
17	MR spectroscopy for in vivo assessment of the oncometabolite 2â€hydroxyglutarate and its effects on cellular metabolism in human brain gliomas at 9.4T. Journal of Magnetic Resonance Imaging, 2016, 44, 823-833.	3.4	36
18	Physics of Hybrid Imaging. , 2016, , 3-12.		0

#	Article	IF	CITATIONS
19	Bone Marrow Lipid Profiles from Peripheral Skeleton as Potential Biomarkers for Osteoporosis: A 1H-MR Spectroscopy Study. Academic Radiology, 2016, 23, 273-283.	2.5	49
20	Diffusion properties of conventional and calciumâ€ s ensitive MRI contrast agents in the rat cerebral cortex. Contrast Media and Molecular Imaging, 2014, 9, 71-82.	0.8	22
21	Functional quantitative susceptibility mapping (fQSM). NeuroImage, 2014, 100, 112-124.	4.2	76
22	Investigation of a Calcium-Responsive Contrast Agent in Cellular Model Systems: Feasibility for Use as a Smart Molecular Probe in Functional MRI. ACS Chemical Neuroscience, 2014, 5, 360-369.	3.5	29
23	Dualâ€Frequency Calciumâ€Responsive MRI Agents. Chemistry - A European Journal, 2014, 20, 7351-7362.	3.3	44
24	E07 Progressive Iron Accumulation In Huntington Disease Basal Ganglia: A Longitudinal Study. Journal of Neurology, Neurosurgery and Psychiatry, 2014, 85, A37-A38.	1.9	0
25	Arylâ€Phosphonate Lanthanide Complexes and Their Fluorinated Derivatives: Investigation of Their Unusual Relaxometric Behavior and Potential Application as Dual Frequency ¹ H/ ¹⁹ Fâ€MRI Probes. Chemistry - A European Journal, 2013, 19, 11644-11660.	3.3	18
26	Effect of <i>r</i> ₁ and <i>r</i> ₂ relaxivity of gadoliniumâ€based contrast agents on the <i>T</i> ₁ â€weighted MR signal at increasing magnetic field strengths. Contrast Media and Molecular Imaging, 2013, 8, 456-465.	0.8	62
27	A smart ¹⁹ F and ¹ H MRI probe with selfâ€immolative linker as a versatile tool for detection of enzymes. Contrast Media and Molecular Imaging, 2012, 7, 478-483.	0.8	37
28	Phase stability in fMRI time series: Effect of noise regression, off-resonance correction and spatial filtering techniques. NeuroImage, 2012, 59, 3748-3761.	4.2	23
29	Metabolic correlatives of brain activity in a FOS epilepsy patient. NMR in Biomedicine, 2010, 23, 170-178.	2.8	14
30	Combined Volumetry and DTI in Subcortical Structures of Mild Cognitive Impairment and Alzheimer's Disease Patients. Journal of Alzheimer's Disease, 2010, 19, 1273-1282.	2.6	107
31	Smoothing that does not blur: Effects of the anisotropic approach for evaluating diffusion tensor imaging data in the clinic. Journal of Magnetic Resonance Imaging, 2010, 31, 690-697.	3.4	15
32	The sign convention for phase values on different vendor systems: definition and implications for susceptibility-weighted imaging. Magnetic Resonance Imaging, 2010, 28, 297-300.	1.8	18
33	<i>In vivo</i> quantification of the bound pool <i>T</i> ₁ in human white matter using the binary spin–bath model of progressive magnetization transfer saturation. Physics in Medicine and Biology, 2009, 54, N529-N540.	3.0	41
34	Volume and iron content in basal ganglia and thalamus. Human Brain Mapping, 2009, 30, 2667-2675.	3.6	98
35	Characterization of white matter fiber bundles with <i>T</i> relaxometry and diffusion tensor imaging. Magnetic Resonance in Medicine, 2009, 61, 1066-1072.	3.0	62
36	Advantages of using multiple-echo image combination and asymmetric triangular phase masking in magnetic resonance venography at 3 T. Magnetic Resonance Imaging, 2009, 27, 23-37.	1.8	23

#	Article	IF	CITATIONS
37	A highly sensitive radial diffusion measurement method for white matter tract investigation. Magnetic Resonance Imaging, 2009, 27, 519-530.	1.8	2
38	Quantification of gray matter changes in the cerebral cortex after isolated cerebellar damage: a voxel-based morphometry study. Neuroscience, 2009, 162, 827-835.	2.3	39
39	The effect of physiological noise in phase functional magnetic resonance imaging: from blood oxygen level-dependent effects to direct detection of neuronal currents. Magnetic Resonance Imaging, 2008, 26, 1026-1040.	1.8	31
40	Structural Correlates of Implicit Learning Deficits in Subjects with Developmental Dyslexia. Annals of the New York Academy of Sciences, 2008, 1145, 212-221.	3.8	41
41	Realistic simulations of neuronal activity: A contribution to the debate on direct detection of neuronal currents by MRI. NeuroImage, 2008, 39, 87-106.	4.2	55
42	Essential Head Tremor Is Associated with Cerebellar Vermis Atrophy: A Volumetric and Voxel-Based Morphometry MR Imaging Study. American Journal of Neuroradiology, 2008, 29, 1692-1697.	2.4	158
43	Multimodal fMRI tractography in normal subjects and in clinically recovered traumatic brain injury patients. NeuroImage, 2007, 34, 1331-1341.	4.2	27
44	Model-free analysis of brain fMRI data by recurrence quantification. NeuroImage, 2007, 37, 489-503.	4.2	25
45	Voxelâ€based analysis of R2* maps in the healthy human brain. Journal of Magnetic Resonance Imaging, 2007, 26, 1413-1420.	3.4	79
46	Implicit learning deficits in dyslexic adults: An fMRI study. NeuroImage, 2006, 33, 1218-1226.	4.2	133
47	Functional changes in the activity of cerebellum and frontostriatal regions during externally and internally timed movement in Parkinson's disease. Brain Research Bulletin, 2006, 71, 259-269.	3.0	121
48	Validation studies on the 5-hydroxy-L-[β-11C]-tryptophan/PET method for probing the decarboxylase step in serotonin synthesis. Synapse, 2006, 59, 521-531.	1.2	19
49	Challenges for detection of neuronal currents by MRI. Magnetic Resonance Imaging, 2006, 24, 483-493.	1.8	54
50	Imaging nervous pathways with MR tractography. Radiologia Medica, 2006, 111, 268-283.	7.7	4
51	Dysfunction of a Structurally Normal Motor Pathway in a Brain Injury Patient as Revealed by Multimodal Integrated Techniques. Neurocase, 2006, 12, 232-235.	0.6	5
52	High-Field Neuroimaging in Traumatic Brain Injury. , 2006, , 169-176.		3
53	High-Field Neuroimaging in Parkinson's Disease. , 2006, , 194-200.		3
54	High-Field 3 T Imaging of Alzheimer Disease. , 2006, , 201-207.		1

4

#	Article	IF	CITATIONS
55	Nerve Pathways with MR Tractography. , 2006, , 79-90.		0
56	The appreciation of wine by sommeliers: a functional magnetic resonance study of sensory integration. NeuroImage, 2005, 25, 570-578.	4.2	90
57	Fast detection of diffuse axonal damage in severe traumatic brain injury: comparison of gradient-recalled echo and turbo proton echo-planar spectroscopic imaging MRI sequences. American Journal of Neuroradiology, 2005, 26, 1140-8.	2.4	21
58	Pulsed saturation of the standard two-pool model for magnetization transfer. Part I: The steady state. Concepts in Magnetic Resonance, 2004, 21A, 37-49.	1.3	15
59	Pulsed saturation of the standard two-pool model for magnetization transfer. Part II: The transition to steady state. Concepts in Magnetic Resonance, 2004, 21A, 50-62.	1.3	9
60	Combination of BOLD-fMRI and VEP recordings for spin-echo MRI detection of primary magnetic effects caused by neuronal currents. Magnetic Resonance Imaging, 2004, 22, 1429-1440.	1.8	40
61	Simultaneous EEG–fMRI acquisition: how far is it from being a standardized technique?. Magnetic Resonance Imaging, 2004, 22, 1445-1455.	1.8	32
62	Visually cued motor synchronization: modulation of fMRI activation patterns by baseline condition. Neuroscience Letters, 2004, 373, 32-37.	2.1	18
63	Evaluation of mixed effects in event-related fMRI studies: impact of first-level design and filtering. NeuroImage, 2004, 22, 1351-1370.	4.2	26
64	Intermolecular double quantum coherences (iDQc) and diffusion-weighted imaging (DWI) imaging of the human brain at 1.5 T. Magnetic Resonance Imaging, 2003, 21, 1151-1157.	1.8	12
65	Quantification of magnetization transfer by sampling the transient signal using MT-prepared single-shot EPI. Concepts in Magnetic Resonance, 2003, 19A, 149-152.	1.3	6
66	Quantitative NumART2* mapping in functional MRI studies at 1.5 T. Magnetic Resonance Imaging, 2003, 21, 1241-1249.	1.8	3
67	Coefficient D(av) is more sensitive than fractional anisotropy in monitoring progression of irreversible tissue damage in focal nonactive multiple sclerosis lesions. American Journal of Neuroradiology, 2003, 24, 663-70.	2.4	37
68	Brain Regions Involved in Fatigue Sensation: Reduced Acetylcarnitine Uptake into the Brain. NeuroImage, 2002, 17, 1256-1265.	4.2	97
69	Real-time quantification ofT2* changes using multiecho planar imaging and numerical methods. Magnetic Resonance in Medicine, 2002, 48, 877-882.	3.0	51
70	In vivo multiple spin echoes imaging of trabecular bone on a clinical 1.5 T MR scanner. Magnetic Resonance Imaging, 2002, 20, 623-629.	1.8	17
71	Kinetic Compartment Modeling of [11C]-5-Hydroxy-L-Tryptophan for Positron Emission Tomography Assessment of Serotonin Synthesis in Human Brain. Journal of Cerebral Blood Flow and Metabolism, 2002, 22, 1352-1366.	4.3	35
72	Kinetic Compartment Modeling of [11C]-5-Hydroxy-L-Tryptophan for Positron Emission Tomography Assessment of Serotonin Synthesis in Human Brain. Journal of Cerebral Blood Flow and Metabolism, 2002, , 1352-1366.	4.3	12

#	Article	IF	CITATIONS
73	Presynaptic serotonin imaging in social phobia using [3-11C]-5-hydroxy-L-tryptophan and PET. NeuroImage, 2001, 13, 1070.	4.2	5
74	Improved Detection of Event-Related Functional MRI Signals Using Probability Functions. NeuroImage, 2001, 14, 1193-1205.	4.2	97
75	Synthesis and Characterization of Binding of 5-[76Br] Bromo-3-[[2(S)-Azetidinyl]methoxy]pyridine, a Novel Nicotinic Acetylcholine Receptor Ligand, in Rat Brain. Journal of Neurochemistry, 2001, 73, 1264-1272.	3.9	22
76	PET with 11 C-deuterium-deprenyl and 18 F-FDG in focal epilepsy. Acta Neurologica Scandinavica, 2001, 103, 360-366.	2.1	62
77	Regulation of dopaminergic activity in early Parkinson's disease. Annals of Neurology, 1999, 46, 359-365.	5.3	37
78	Increased dopamine synthesis rate in medial prefrontal cortex and striatum in schizophrenia indicated by L-(β-11C) DOPA and PET. Biological Psychiatry, 1999, 46, 681-688.	1.3	267
79	From magnetic resonance spectroscopy to classification of tumors. A review of pattern recognition methods. , 1998, 11, 148-156.		97
80	N-[11C]Methylspiperone PET, in contrast to [11C]raclopride, fails to detect D2 receptor occupancy by an atypical neuroleptic. Psychiatry Research - Neuroimaging, 1998, 82, 147-160.	1.8	30
81	Assignment of glial brain tumors in humans byin vivo 1H-magnetic resonance spectroscopy and multidimensional metabolic classification. Magnetic Resonance Materials in Physics, Biology, and Medicine, 1997, 5, 179-183.	2.0	16
82	Proton chemical shift imaging, metabolic maps, and single voxel spectroscopy of glial brain tumors. Magnetic Resonance Materials in Physics, Biology, and Medicine, 1996, 4, 139-150.	2.0	36
83	Proton MRS of Gadolinium-enhancing MS Plaques and Metabolic Changes in Normal-Appearing White Matter. Magnetic Resonance in Medicine, 1995, 33, 811-817.	3.0	54
84	In Vivo proton MR spectroscopy of human gliomas: definition of metabolic coordinates for multi-dimensional classification. Magnetic Resonance in Medicine, 1995, 34, 242-252.	3.0	68
85	Phase Variations in fMRI Time Series Analysis: Friend or Foe?. , 0, , .		2